Interaction of Guanine Nucleotides with the Signal Recognition Particle from *Escherichia coli*†

Junutula R. Jagath, Marina V. Rodnina, Georg Lentzen, and Wolfgang Wintermeyer*

Institute of Molecular Biology, University of Witten/Herdecke, 58448 Witten, Germany

Received June 26, 1998

ABSTRACT: The bacterial signal recognition particle (SRP) is an RNA−protein complex. In *Escherichia coli*, the particle consists of a 114 nt RNA, a 4.5S RNA, and a 48 kDa GTP-binding protein, Ffh. GDP−GTP exchange on, and GTP hydrolysis by, Ffh are thought to regulate SRP function in membrane targeting of translating ribosomes. In the present paper, we report the equilibrium and kinetic constants of guanine nucleotide binding to Ffh in different functional complexes. The association and dissociation rate constants of GTP/GDP binding to Ffh were measured using a fluorescent analogue of GTP/GDP, mant-GTP/GDP. For both nucleotides, association and dissociation rate constants were about 10^6 M^{-1} s^{-1} and 10 s^{-1}, respectively. The equilibrium constants of nonmodified GTP and GDP binding to Ffh alone and in SRP, and in the complex with the ribosomes were measured by competition with mant-GDP. In all cases, the same 1−2 μM affinity for GTP and GDP was observed. Binding of both GTP and GDP to Ffh was independent of Mg^{2+} ions. The data suggest that, at conditions *in vivo*, (i) there will be rapid spontaneous GDP−GTP exchange, and (ii) the GTP-bound form of Ffh, or of SRP, will be predominant.

The signal recognition particle (SRP) is an RNA−protein complex that functions in cotranslational membrane targeting of ribosomes carrying nascent presecretory proteins with a hydrophobic signal sequence at the N terminus (*1*, *2*). SRP-like RNPs have been characterized in mammals, yeast, prokaryotes, and organelles and are probably present in all organisms. While mammalian SRP consists of a 300 nt RNA, a 7S RNA, and six different proteins, *Escherichia coli* SRP is much simpler, being composed of a smaller 114 nt RNA, a 4.5S RNA, and one 48 kDa protein, Ffh (or P48) (*3*, *4*). Ffh, like its eukaryotic homologue, SRP54, is a GTPase which consists of three structural domains: the N-terminal N domain, the GTP-binding domain, and the C-terminal methionine-rich M domain. The M domain binds SRP RNA as well as the signal peptide emerging from the ribosome (*5*, *6*), while the G domain is thought to regulate, by GTP binding and hydrolysis, Ffh-mediated interactions of SRP with the signal peptide and the ribosomes as well as with the SRP receptor at the membrane.

The SRP receptor in *E. coli* is FtsY (*7*), the homologue of the mammalian SRP receptor, SRα, which functions in a complex with SRβ (*8*). SRP receptors are GTPases that are homologous to SRP54 proteins with respect to both specific features of the G domain and the presence of the adjacent N domain, features which define the subfamily of SRP-related GTPases (*9*). The recently determined crystal structures of the nucleotide-free NG domains of *Thermus aquaticus* Ffh (*10*) and *E. coli* FtsY (*11*) are remarkably similar and, as discussed below, the two proteins indeed have similar GTP/GDP binding properties.

The paradigm established for a number of GTPases is that activation, by exchange of bound GDP with GTP, is regulated by guanine nucleotide release proteins (GNRP). Well-documented examples are Ras and EF-Tu, where the respective GNRPs, Sos, and EF-Ts, are well characterized. In those cases, GDP is very tightly bound in the absence of the GNRP and is released only from the GTPase−GNRP complex to allow subsequent binding of GTP which is present at a concentration about 10 times higher than that of GDP in vivo. The crystal structures of the EF-Tu-EF-Ts complexes from *E. coli* (*12*) and *T. thermophilus* (*13*) are known and suggest how EF-Ts changes the nucleotide-binding site of EF-Tu to promote GDP release. There are other GTPases where GDP−GTP exchange takes place spontaneously; examples are the translational factors, IF2, EF-G, and RF3, for which no GNRP has been found. Similarly, no GNRPs have been found for SRP-related GTPases, although increased cross-linking of GTP to SRP54 in mammalian SRP upon binding to ribosomes has been reported, indicating a function of the ribosome in regulating nucleotide uptake by SRP (*14*).

SRP-mediated membrane targeting of translating ribosomes requires GTP binding and hydrolysis on both SRP54 (Ffh) and SRα (FtsY) (*1*). Exactly how GTP binding and hydrolysis are regulated and drive the process is not known. Results available for the eukaryotic system suggest that nucleotide-free SRP binds to the signal peptide emerging from the ribosome and subsequently to the SRP receptor. Tightening of the SRP−SRα complex by GTP binding has been reported (*15*). Subsequent to signal peptide transfer to the translocon (Sec61), GTP hydrolysis on both SRP and SRα (*16*) in a "concerted switch"-type mechanism (*15*, *17*) weakens the interaction, thereby allowing the dissociation of the SRP−SRα complex and the recycling of SRP.

† This work was supported by the Deutsche Forschungsgemeinschaft (Wi 626/6-2), the Alfried Krupp von Bollen und Halbach-Stiftung, and the Fonds der Chemischen Industrie. J.R.J. acknowledges a fellowship of the Alexander von Humboldt-Stiftung.

* Corresponding author. Tel: (49-2302) 669-140. Fax: (49-2302) 669-117. E-mail: winterme@uni-wh.de.

10.1021/bi981523a CCC: $15.00
Published on Web 10/14/1998

Much less is known for the prokaryotic system. Evidence has been presented suggesting the reciprocal stimulation of GTP hydrolysis by Ffh and FtsY (*18*, *19*), in keeping with a similar situation with the eukaryotic homologues (*16*). Quantitative data on GTP/GDP binding are available for *E. coli* FtsY (*20*); for Ffh, the K_M value for GTP measured by GTP hydrolysis has been reported (*19*).

Here we report a study on both kinetics and equilibrium of the interaction of guanine nucleotides with *E. coli* Ffh and its complexes with 4.5S RNA and ribosomes. Kinetics of nucleotide binding to Ffh were measured by stopped flow, monitoring the increase of the fluorescence of mant derivatives of GTP or GDP. Equilibrium binding of unmodified nucleotides was measured by competition with mant-GDP.

MATERIALS AND METHODS

Materials. Ni-NTA-Agarose was obtained from Qiagen. 2′-(or-3′)-*O*-(*N*-Methylanthraniloyl)guanosine 5′-diphosphate (and -triphosphate) (mant-GDP and mant-GTP) were purchased from Molecular Probes. GTP and GDP were purchased from Boehringer Mannheim. All other chemicals used in this study were obtained from Merck or Sigma. Centricon filters were from Amicon.

Preparation of Ffh, 4.5S RNA, SRP, and 70S Ribosomes. The plasmid pET-21-Ffh(His-6) coding for Ffh extended by eight amino acids including six histidines at the C-terminus was coexpressed with a 4.5S RNA expressing plasmid pACYC-ffs in *E. coli* JM109(DE3) (Lentzen et al., manuscript in preparation). Ffh protein was purified by Ni-NTA-Agarose affinity chromatography as described by Lentzen et al. (*21*) with the following modifications. The cell pellet (5 g, wet weight) was suspended in 100 mL of extraction buffer (50 mM sodium phosphate, pH 8.0, 0.7 M sodium chloride, 0.1 mM EDTA, 1% Triton X-100, 10 mM 2-mercaptoethanol, 1 mM phenyl methylsulfonyl fluoride), and the suspension was sonicated for 30 min (Branson Sonifier). The extract was centrifuged at 20000*g* for 20 min, and the supernatant obtained was loaded onto a Ni-NTA-Agarose column (1 cm^2 × 10 cm) which was pre-equilibrated with Buffer A (50 mM sodium phosphate, pH 8.0, 0.7 M sodium chloride, 10 mM 2-mercaptoethanol, 10% v/v glycerol). After washing the column with 400 mL of 80% Buffer A and 20% Buffer B (50 mM sodium phosphate, pH 7.0, 0.7 M sodium chloride, 10 mM 2-mercaptoethanol, 10% glycerol, 150 mM imidazol), Ffh was eluted with 100% Buffer B. Ffh-containing fractions were pooled and concentrated with 30 kDa Centricon filters. Protein concentration was determined by the Bradford method using bovine serum albumin as a standard (*22*). The purity of the protein was more than 90% as judged from SDS−polyacrylamide gel electrophoresis analysis. 4.5S RNA was transcribed in vitro using as a template a linearized plasmid with T7 polymerase; the transcript was purified by FPLC on MonoQ (Pharmacia). Ribosomes (70S) from *E. coli* MRE600 were prepared as described (*23*). SRP was reconstituted by incubating Ffh and 4.5S RNA in a 1:2 molar ratio for 5 min at 25 °C.

Analysis of GTP/GDP Content of Ffh. The absence of bound nucleotide in purified Ffh was verified by HPLC analysis. The column (ET 125/8/4 Nucleosil 120-3 C_{18} MPN) was equilibrated with 65 mM potassium phosphate, pH 6.2, 2 mM tetrabutylammonium hydrogen sulfate, and 15% acetonitril. GTP and GDP were used as standards. One volume (10 μL of 60 μM stock) of Ffh was mixed with 4 volumes (40 μL) of HPLC column equilibration buffer and 1 volume (10 μL) of 1 M potassium phosphate, pH 6.5, and mixed for 5 min followed by 5 min of centrifugation at 12 000 rpm. The supernatant was diluted with the same volume of HPLC equilibration buffer. This sample (50 μL) was subjected to HPLC analysis. According to the analysis, the Ffh used for the present experiments was free of GTP and GDP.

Fluorescence Measurements and Chase Titrations. Fluorescence emission spectra were recorded at 20 ± 2 °C in quartz cuvettes (i.d., 4 mm × 4 mm) on a Schoeffel RRS 1000 spectrofluorimeter upon excitation at 360 nm. The following buffer was used (buffer C): 50 mM Tris-HCl, pH 7.5, 70 mM ammonium chloride, 30 mM potassium chloride, 7 mM magnesium chloride, and 1 mM dithiothreitol.

Binding of mant-GTP and mant-GDP to Ffh was monitored by fluorescence measurements using excitation and emission wavelengths of 360 and 438 nm, respectively. Buffer and temperature used for the measurements were the same as above, if not stated otherwise. To estimate the K_d of the complexes, the fluorescence of 0.75 μM mant-GDP was measured alone and with increasing amounts (up to 10 μM) of Ffh or SRP, in the absence and presence of an equimolar excess of 70S ribosomes. The resulting fluorescence was corrected for dilution and for background fluorescence. The data were evaluated by fitting according to the formalism described previously (*24*).

The chase of mant-GDP from Ffh (or SRP, or the respective ribosome complexes) by GTP or GDP was measured using 0.5 μM each of mant-GDP and Ffh (or the respective complex), and increasing concentrations of unmodified nucleotide. For analyzing the chase titration data, the following model was used:

$$P + A \overset{K_A}{\leftrightarrow} AP$$

$$P + I \overset{K_I}{\leftrightarrow} PI$$

where P, Ffh (or the respective complex); A, mant-GDP; I, GTP or GDP; K_A and K_I, equilibrium dissociation constants of A and I, respectively. The conditions (see Figure 3) were chosen such that the following assumption was valid: [I] ≫ [A] or [P], and therefore [I] ≅ [I_o].

The solution for [AP] gives

$$[AP] = 0.5(K_A[I]/K_I + K_A + [A_0] + [P_0]) - 0.5\sqrt{(K_A[I]/K_I + K_A + [A_0] + [P_0])^2 - 4[A_0][P_0]}$$

and hence the fluorescence observed in the presence of a competitor I, $F(I)$, is given by

$$F(I) = F(A)([A_0] - [AP]) + F(AP)[AP]$$

where $F(A)$ and $F(AP)$ represent the respective fluorescence intensities of mant-GDP and mant-GDP−Ffh (or the respective Ffh complex). K_I, the equilibrium dissociation constant of the unmodified nucleotide, was calculated by fitting the above equations to the titration data using the Table Curve software (Jandel Scientific).

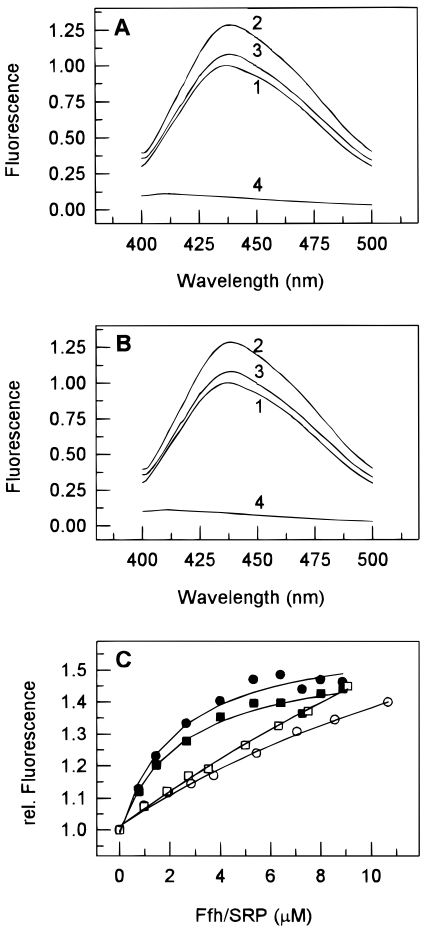

FIGURE 1: Fluorescence changes induced by Ffh binding of mant-GTP (A) or mant-GDP (B). (A) Emission spectra of 0.5 μM mant-GTP (1), after addition of 4.8 μM Ffh (2), and of 140 μM GTP (3); buffer blank (4). (B) Emission spectra of 0.75 μM mant-GDP (1), after addition of 4.8 μM of Ffh (2) and of 140 μM GDP (3); buffer blank (4). (C) Titration of mant-GDP (0.75 μM) with Ffh (○, ●) or SRP (□, ■) in the absence (○, □) and presence (●, ■) of equimolar (0−10 μM) concentrations of ribosomes.

Stopped-Flow Kinetic Experiments. Fluorescence stopped-flow measurements were performed and the data evaluated as described previously (*24*). The fluorescence of mant-GTP and mant-GDP was excited at 363 nm and measured after passing KV408 filters (Schott). The data were evaluated by fitting an exponential function with the characteristic time constant, k_{app}, the amplitude, *A*, and another variable for the final signal. With the apparatus used, time constants of up to 500 s^{-1} could be measured.

Experiments were performed in buffer C at 20 °C by rapidly mixing equal volumes (60 μL each) of the reactants. The reproducibility of the rate constants was 15% or better.

RESULTS

Interaction of mant-GTP and mant-GDP with Ffh. Upon binding to Ffh, the fluorescence of both mant-GTP and mant-GDP increased without a significant shift of the emission maximum (438 nm) (Figure 1A,B). The binding was specific, since addition of the respective unmodified nucleotide in excess largely reversed the effect (Figure 1A,B), whereas ATP or ADP had no effect (not shown). On the basis of the equilibrium binding constants of mant-GTP and mant-GDP determined kinetically (about 8 μM; see below), approximately 25% of mant nucleotide was bound at the concentration of Ffh present in the experiment (4.8 μM). Thus, from the observed 25% fluorescence increase at 25% saturation (Figure 1A), the fluorescence of Ffh-bound mant nucleotides is estimated to be about twice that of the free nucleotides.

Table 1: Kinetic Constants of Mant-GTP/GDP Interaction with Ffh

nucleotide	k_1 (M^{-1} s^{-1})	k_{-1} (s^{-1})	K_d (μM)
mant-GTP	$(0.9 \pm 0.2) \times 10^6$	7.6 ± 0.2	8.2 ± 2.3
mant-GDP	$(1.6 \pm 0.2) \times 10^6$	13.7 ± 0.6	8.5 ± 1.1

To estimate the K_d of the interaction of mant-GDP with Ffh in different functional complexes, titrations were performed at a constant concentration of mant-GDP and increasing concentrations of Ffh or SRP, both in the absence and presence of ribosomes (Figure 1C). Upon addition of Ffh or SRP up to about 8 μM, a practically linear increase in mant-GDP fluorescence was observed. From the curves of Figure 1C, the K_d of mant-GDP−Ffh or mant-GDP−SRP complexes was estimated to be >5 μM, consistent with the value determined kinetically (see below). In the presence of the ribosomes, the affinity of mant-GDP for Ffh and SRP was somewhat higher, 2.2 ± 0.5 and 2.4 ± 0.5 μM, respectively.

The kinetics of binding of both mant-GTP and mant-GDP to Ffh were measured by stopped flow, monitoring the increase of mant fluorescence due to complex formation (Figure 2). Upon increasing the concentration of Ffh, both the amplitude of the fluorescence increase and the rate of complex formation increased. The stopped-flow traces were evaluated by fitting a single-exponential function (pseudo-first-order condition), yielding time constants, k_{app}, and amplitudes for each concentration (Figure 2A,C). From the linear plots of k_{app} versus Ffh concentration (Figures 2B,D), the rate constants for association and dissociation, k_1 and k_{-1}, were determined (Table 1). k_1 and k_{-1} are similar for the two nucleotides within a factor of 2; K_d values calculated from the kinetic constants are the same for mant-GTP and mant-GDP. Thus, both nucleotides bind to Ffh with moderate affinity and dissociate rapidly. The comparison of the K_d values measured for mant-substituted nucleotides with those of unmodified GTP or GDP (see below) reveals that the mant group lowers the affinity up to about 7-fold.

GTP/GDP Binding to Ffh, SRP, and Their Ribosome Complexes. The equilibrium constants of GTP and GDP binding to Ffh were determined by titrating the complex Ffh−mant-GDP with the respective unlabeled nucleotide and following the chase of mant-GDP out of the complex by the decrease of the fluorescence signal (Figure 3). Mant-GDP was chosen as an indicator to avoid any complication introduced by the intrinsic GTPase activity of Ffh (*18*), the rate of which was about 0.07 min^{-1} under the present assay conditions (data not shown). In chase titrations with excess GTP, the extent of GTP hydrolysis by Ffh was negligible, that is, less than 3% of added GTP. Chase titrations (Figure 3) were evaluated as described in Materials and Methods, and the resulting equilibrium constants are summarized in Table 2. For fitting, the K_d value for mant-GDP−Ffh was taken from the kinetic experiments (8.5 μM). The same value was used for mant-GDP−SRP, since very similar titration curves were obtained for the two complexes in the

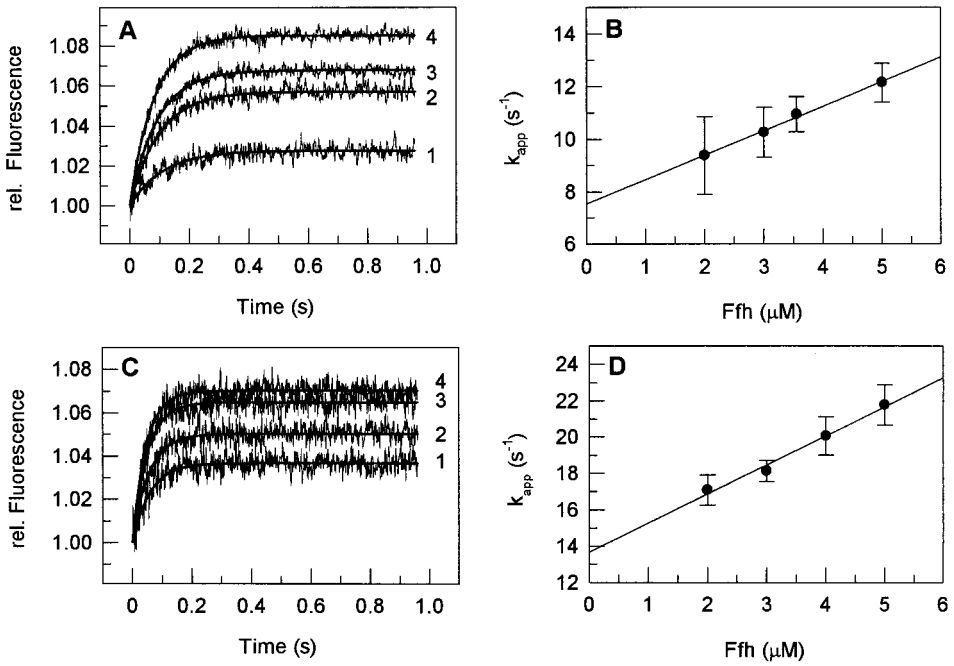

FIGURE 2: Fluorescence stopped-flow kinetics of mant-GTP and mant-GDP binding to Ffh. (A) Time course of the binding of mant-GTP (0.5 μM) to Ffh present in 2 μM (1), 3 μM (2), 3.55 μM (3), and 5 μM (4) concentrations. Traces shown are averaged from 5−8 individual experiments. The smooth lines represent single-exponential fits to the data that yield the respective time constants, k_{app}. (B) Concentration dependence of k_{app} values for mant-GTP. The slope of the fitted straight line yields k_1, and the *y*-axis intercept k_{-1} (Table 1). (C) Time course of the association of mant-GDP (0.75 μM) and Ffh present in 2 μM (1), 3 μM (2), 4 μM (3), and 5 μM (4) concentrations. k_{app} values were obtained as in A. (D) Concentration dependence of k_{app} values for mant-GDP from C. Values of k_1 and k_{-1} obtained from the plot are shown in Table 1.

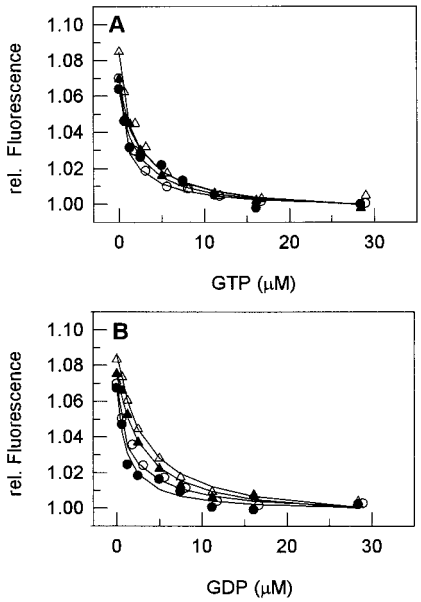

FIGURE 3: Interaction of GTP/GDP with Ffh or SRP in the presence and absence of ribosomes. Ffh (0.5 μM) was mixed with 0.5 μM mant-GDP in the presence (●) and absence (○) of 1.5 μM of ribosomes, and chase titrations were carried out with either GTP (A) or GDP (B). Analogous chase titrations were carried out with 0.5 μM SRP−mant-GDP complex in the presence (▲) and absence (△) of 1.5 μM ribosomes. Solid lines represent the results of the fits, as described in Materials and Methods

equilibrium titration experiments (Figure 1C). Upon addition of ribosomes, the affinity of mant-GDP for Ffh and SRP increased to 2.2−2.4 μM (Figure 1C); these values were used for the evaluation of the respective chase titrations. The K_d values obtained for nonmodified GTP and GDP are the same (1.2−1.3 μM), which shows that the two nucleotides bind to Ffh with the same affinity (Table 2). The addition of 4.5S RNA to Ffh under conditions where at least 80% of the Ffh is bound to form SRP had only a slight influence, if any, on the binding affinity of GTP or GDP (K_d = 1.6−2.3 μM).

Table 2: Equilibrium Dissociation Constants of Different Functional Ffh-GTP/GDP Complexes

complex	K_d (μM)	
	GTP	GDP
Ffh	1.2 ± 0.2	1.3 ± 0.2
SRP	1.6 ± 0.3	2.3 ± 0.5
Ffh-ribosomes	1.2 ± 0.6	1.4 ± 0.3
SRP-ribosomes	1.7 ± 0.2	0.9 ± 0.2

Both free Ffh and Ffh−4.5S RNA form a complex with ribosomes, as shown by gel filtration; at the concentrations used for the nucleotide-binding experiments, 70% of Ffh (or Ffh−4.5S RNA complex) was bound to the ribosomes (data not shown). The affinities of ribosome−Ffh and ribosome−SRP complexes for nonmodified GTP and GDP (about 1−2 μM) were similar to those of Ffh and SRP (Figure 1C). This suggests that complex formation with ribosomes had no effect on GTP or GDP binding to Ffh or Ffh−4.5S RNA (Table 2).

Influence of Mg^{2+} on Guanine Nucleotide Binding to Ffh. Nucleoside di- and triphosphates usually bind to their binding site as Mg^{2+} complexes, and in several crystal structures, direct or water-mediated interactions of the Mg^{2+} ion with nearby amino acid residues have been identified which contribute to the affinity of nucleotide binding. To assess the contribution of Mg^{2+} ions to the affinity of GTP/GDP binding to Ffh, chase titrations as described above (Figure 3) were performed at different Mg^{2+} concentrations. As

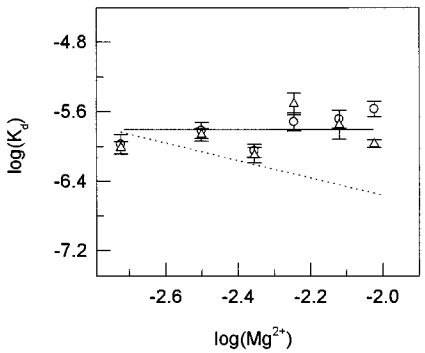

FIGURE 4: Mg^{2+} dependence of GTP/GDP binding to Ffh. GTP/GDP chase titrations were carried out as described in Figure 3 using 0.5 μM Ffh−mant-GDP complex in buffer C containing 0−15 mM Mg^{2+}; an additional experiment was carried out upon addition of 5 mM EDTA to the buffer without Mg^{2+}. K_d values were determined by fitting as described in Materials and Methods. The log values of K_d versus Mg^{2+} concentration are plotted for GTP (○) and GDP (△). The values for K_d for GTP and GDP in buffer containing 5 mM EDTA were 2.3 ± 0.9 μM (log(K_d) = −5.64) and 2.9 ± 0.3 μM (log(K_d) = −5.54), respectively. The dotted line depicts the slope expected if one Mg^{2+} ion contributed to GTP/GDP binding to Ffh.

shown in Figure 4, the affinities of GTP or GDP binding to Ffh were independent of the concentration of added Mg^{2+}. The binding was not significantly affected even by the addition of 5 mM EDTA. These results show that Mg^{2+} does not contribute to the affinity of guanine nucleotide binding to Ffh.

DISCUSSION

Guanine nucleotide-binding proteins differ widely with respect to their nucleotide-binding properties. There are examples of very high affinities with K_d values in the order of 10^{-11}−10^{-12} M, such as Ras (*25*) and Ran (*26*), high affinities around 10^{-9} M (EF-Tu-GDP (*27*, *28*), and moderate affinities of 10^{-6}−10^{-7} M, including GTP binding to EF-Tu (*27*, *28*) and GTP/GDP binding to EF-G (*29*−*31*). The K_m of GTP binding to the Ffh−4.5S RNA complex, measured by GTP hydrolysis, was reported to be about 0.7 μM (25 °C) (*19*). For the isolated NG domain of FtsY, K_d values for GTP and GDP binding have been reported to be 10 and 2 μM (20 °C), respectively (*20*). The present values obtained for Ffh, 1−2 μM (20 °C) for both GTP and GDP, are in that range, although the affinity of GTP binding to Ffh is significantly higher. The dissociation rate constants are also similar for the GTP/GDP complexes of FtsY, about 4 s^{-1} (*20*), and Ffh, about 10 s^{-1} (this paper), thus obviating the need of a nucleotide exchange factor for the two proteins.

The similarity of nucleotide binding is in keeping with the structural homology of the NG domains (comprising the G domain and the N domain) of Ffh and FtsY, as revealed by the crystal structures (*10*, *11*). The G domains of Ffh and FtsY are distinguished from the G domains of other GTPases, such as Ras, Gα, or EF-Tu, by the insertion into the effector loop of a stretch of amino acids, referred to as I box, that folds into a βαβα (Ffh) (*10*) or αβα (FtsY) (*11*) structure and contains the G2 motif of the nucleotide-binding site. The other distinguishing feature that FtsY and Ffh have in common is the four-helix N domain that tightly packs against the G domain at the side opposite to the I box. Both features are likely to determine the nucleotide-binding properties of the two proteins and may cause the nucleotide-binding site of nucleotide-free Ffh and FtsY to be wide open (*10*, *11*).

The kinetic data show that the second-order rate constant of binding of both mant-GTP and mant-GDP is in the order of 10^6 M^{-1} s^{-1}, much lower than expected for the diffusion-controlled formation of an encounter complex. It is likely, therefore, that the low association rate constant reflects a conformational change that follows the formation of the encounter complex, which itself does not lead to an observable signal change. The binding of unmodified nucleotides is most likely similar. Thus, the nucleotide-binding mechanisms of Ffh and FtsY (*20*) resemble each other in that the rate-limiting step is a conformational change following diffusion-controlled binding. It is likely that the slow binding reflects the necessity for the nucleotide-binding pocket to close to allow the nucleotide to establish binding interactions, as has been proposed for FtsY (*20*).

In several GTP-binding proteins, like EF-Tu and Ras, GTP/GDP in the active site is bound as a complex with a Mg^{2+} ion that stabilizes the binding. Nucleotide exchange, that is, the dissociation of GDP and binding of GTP, in these cases requires the interaction with a GNRP, EF-Ts and Sos, for EF-Tu and Ras, respectively. The crystal structure of the EF-Tu-EF-Ts complex from *E. coli* suggests that EF-Ts acts by destabilizing the Mg^{2+} ion, thereby promoting GDP dissociation (*12*). For Ffh, the present results show that Mg^{2+} does not contribute to the affinity of GTP/GDP binding. Thus, either the nucleotide binds without Mg^{2+} or nucleotide-bound Mg^{2+} is not involved in strong binding interactions with the protein. This may be another reason for the lability of the complex of Ffh with GTP/GDP.

Rapid spontaneous exchange of nucleotides on Ffh in SRP means that at the intracellular concentrations of GTP and GDP in vivo, around 900 and 100 μM, respectively (*32*), SRP will be present in the nucleotide-bound form, predominantly in the GTP-bound form. It seems unlikely, therefore, that nucleotide-free *E. coli* SRP is functional in ribosome binding and protein targeting to the membrane, in particular, since the interaction of *E. coli* SRP with ribosomes has no influence on nucleotide binding at equilibrium. This may be different in the eukaryotic system where a stimulation of GTP binding to SRP upon binding to ribosomes has been observed by UV-induced cross-linking (*14*). Equilibrium binding studies with *E. coli* SRP and nascent-chain ribosomes have to be carried out, however, before a final conclusion with respect to an influence of the ribosome on nucleotide binding of SRP can be reached. As to GDP−GTP exchange at a later stage of the SRP cycle, it is possible that it is inhibited when SRP is bound to the receptor, FtsY. The interaction has been reported to stimulate GTP hydrolysis on both SRP and FtsY (*18*, *19*), and in the homologous eukaryotic SRP−SRα complex, nucleotide binding is stabilized (*15*). The approach described in the present report will be useful to address the open questions in the more complete prokaryotic system consisting of SRP, FtsY, and the ribosome.

ACKNOWLEDGMENT

We thank Petra Striebeck and Jutta Heinemann for expert technical assistance, and Dmitri Rodnin for programming.

REFERENCES

1. Walter, P., and Johnson, A. E. (1994) *Annu. Rev. Cell Biol. 10*, 87−119.
2. Rapoport, T. A., Jungnickel, B., and Kutay, U. (1996) *Annu. Rev. Biochem. 65*, 271−303.
3. Poritz, M. A., Bernstein, H. D., Strub, K., Zopf, D., Wilhelm, H., and Walter, P. (1990) *Science 250*, 1111−1117.
4. Ribes, V., Römisch, K., Giner, A., Dobberstein, B., and Tollervey, D. (1990) *Cell 63*, 591−600.
5. Römisch, K., Webb, J., Lingelbach, K., Gausepohl, H., and Dobberstein, B. (1990) *J. Cell Biol. 111*, 1793−1802.
6. Zopf, D., Bernstein, H. D., and Walter, P. (1993) *J. Cell Biol. 120*, 1113−1121.
7. Luirink, J., ten Hagen-Jongman, C. M., Van der Weijden, C. C., Oudega, B., High, S., Dobberstein, B., and Kusters, R. (1994) *EMBO J. 13*, 2289−2296.
8. Miller, J. D., Tajima, S., Lauffer, L., and Walter, P. (1995) *J. Cell Biol. 128*, 273−282.
9. Bourne, H. R., Sanders, D. A., and McCormick, F. (1991) *Nature 349*, 117−127.
10. Freymann, D. M., Keenan, R. J., Stroud, R. M., and Walter, P. (1997) *Nature 385*, 361−364.
11. Montoya, G., Svensson, C., Luirink, J., and Sinning, I. (1997) *Nature 385*, 365−368.
12. Kawashima, T., Berthet-Colominas, C., Wulff, M., Cusack, S., and Leberman, R. (1996) *Nature 379*, 511−518.
13. Wang Y., Jiang Y., Meyering-Voss M., Sprinzl M., and Sigler P. B. (1997) *Nat. Struct. Biol. 4*, 650−656.
14. Bacher, G., Lütcke, H., Jungnickel, B., Rapoport, T. A., and Dobberstein, B. (1996) *Nature 381*, 248−251.
15. Rapiejko, P. J., and Gilmore, R. (1997) *Cell 89*, 703−713.
16. Miller, J. D., Wilhelm, H., Gierasch, L., Gilmore, R., and Walter, P. (1993) *Nature 366*, 351−354.
17. Milman, J., and Andrews, D. W. (1997) *Cell 89*, 673−676.
18. Miller, J. D., Bernstein, H. D., and Walter, P. (1994) *Nature 367*, 657−659.
19. Powers, T., and Walter, P. (1995) *Science 269*, 1422−1424.
20. Moser, C., Mol, O., Goody, R. S., and Sinning, I. (1997) *Proc. Natl. Acad. Sci. U.S.A. 94*, 11339−11344.
21. Lentzen, G., Dobberstein, B., and Wintermeyer, W. (1994) *FEBS Lett. 348*, 233−238.
22. Bradford, M. M. (1976) *Anal. Biochem. 72*, 248−254.
23. Rodnina, M. V., and Wintermeyer, W. (1995) *Proc. Natl. Acad. Sci. U.S.A. 92*, 1945−1949.
24. Rodnina, M. V., Pape, T., Fricke, R., Kuhn, L., and Wintermeyer, W. (1996) *J. Biol Chem. 271*, 646−652.
25. John, J., Sohmen, R., Feuerstein, J., Linke, R., Wittinghofer, A., and Goody, R. S. (1990) *Biochemistry 29*, 6058−6065.
26. Klebbe, C., Prinz, H., Wittinghofer, A., and Goody, R. S. (1995) *Biochemistry 34*, 12543−12552.
27. Arai, K., Kawakita, M., and Kaziro, Y. (1982) *J. Biochem. 76*, 293−306.
28. Fasano, O., Crechet, J. B., and Parmeggiani, A. (1982) *Anal. Biochem. 124*, 53−58.
29. Rohrbach, M. S., and Bodley, J. W. (1976) *Biochemistry 15*, 4565−4569.
30. Baca, O. G., Rohrbach, M. S., and Bodley, J. W. (1976) *Biochemistry 15*, 4570−4574.
31. Kaziro Y. (1978) *Biochim. Biophys. Acta* 505, 95−127.
32. Neuhard, J., and Nygaard, P. (1987) in *Escherichia coli and Salmonella typhimurium* (Neidhardt, K. C., Ed.) pp 445−473, American Society of Microbiology, Washington, D.C.

BI981523A